Journal of Power Sources 210 (2012) 402–408

Contents lists available at ScienceDirect

Journal of Power Sources

journal homepage: www.elsevier.com/locate/jpowsour

Evaluating kinetic models for preferential CO-oxidation catalysts using optimization-based parameter estimation

Adam C. Baughman[a,b], Xinqun Huang[c], Lealon L. Martin[a,b,d,*]

[a] Department of Chemical and Biological Engineering, Rensselaer Polytechnic Institute, 110 Eighth Street, Troy, NY 12180, USA
[b] Center for Biotechnology and Interdisciplinary Studies, Rensselaer Polytechnic Institute, 110 Eighth Street, Troy, NY 12180, USA
[c] Covidien, 3600 North Second Street, St. Louis, MO 63147, USA
[d] Department of Chemical Engineering, University of Texas Austin, 1 University Station C0400, Austin, TX 78712 USA

ARTICLE INFO

Article history:
Received 11 November 2010
Received in revised form 13 January 2011
Accepted 13 January 2011
Available online 5 March 2011

Keywords:
Reactor modeling
Process optimization
Hydrogen production

ABSTRACT

We adapt a general-purpose optimization-based parameter estimation technique previously described in the literature [1] to evaluate the suitability of a number of common kinetic models for the representation of key performance characteristics (conversion and selectivity) of catalysts used for the preferential oxidation of CO in the presence of H_2. We find that, for process engineering applications, there is no clear practical advantage to using mechanistically based kinetic models (e.g. Langmuir–Hinshelwood) unless the precise chemical mechanism is known. Empirical rate models are found generally to provide equivalent or better simulations of key performance variables for a diverse group of catalyst formulations. Furthermore, we demonstrate that the water–gas-shift (WGS) reaction is relevant within PROX reaction systems under conditons containing high fractions of CO_2 and H_2, confirming the expectations of Choi and Stenger (2004) [2]. Finally, we attempt to identify any emergent trends in kinetic parameters among catalysts sharing similar active metal or metal oxide components. Unfortunately, apart from confirming that the activation barrier for CO oxidation is generally less than the barrier for H_2 oxidation (an expected relationship for PROX catalysts), no such trends are found.

1. Introduction

Noble metals (platinum and palladium, in particular) and noble metal alloys (platinum/ruthenium blends) remain the anode catalyst of choice in state-of-the-art polymer–electrolyte–membrane (PEM) fuel-cell devices. This is because no other material has yet been shown to provide equivalent electrochemical performance [3]. Unfortunately, noble metal catalysts are well known to be susceptible to poisoning by both sulfur and carbon monoxide, especially at lower temperatures (<100 °C). Therefore, to both extend the useful life of the fuel-cell device and to reduce the materials cost associated with replacing expensive noble metal electrodes, it is crucial ensure that catalyst poisoning is minimized. The exact amount of carbon monoxide that can be tolerated for fuel cell applications varies with the amount of precious metal used and with the operating temperature of the device, but is typically less than 10 ppm for PEM fuel cells.

It is estimated that 80% of the hydrogen produced worldwide comes from the reforming of methane and other light hydrocarbons. The hydrogen-rich gaseous mixture produced by such reforming processes typically contains between 80,000 and 120,000 ppm (8–12%) carbon monoxide. The carbon monoxide content is often reduced (and hydrogen content simultaneously enriched) using a follow-on water–gas-shift reaction, but the amount of carbon monoxide in the final product stream is typically about 10,000 ppm (1%).

The preferential (or selective) catalytic oxidation of carbon monoxide to carbon dioxide (PROX) is considered to be an economical and highly distributable process for the removal of trace amounts of carbon monoxide. A large number of catalyst formulations for this process have been described in the literature, most of which involve noble metals (platinum, palladium, ruthenium, or rhodium) as the active element. In the case of PROX processes, noble metal catalyst poisoning by carbon monoxide is less of a concern, as the reactors typically operate at moderately high temperatures (between 150 °C and 250 °C).

In the present work, we leverage a robust general-purpose optimization-based parameter estimation technique previously described in the literature [1] to evaluate the suitability of different kinetic models for the accurate simulation of PROX catalyst performance characteristics: specifically the overall CO conversion

* Corresponding author at: Center for Biotechnology and Interdisciplinary Studies, Rensselaer Polytechnic Institute, 110 Eighth Street, Troy, NY 12180, USA.
Tel.: +1 518 276 3327; fax: +1 518 274 4030.
E-mail address: llmartin@che.utexas.edu (L.L. Martin).

0378-7753/$ – see front matter © 2012 Published by Elsevier B.V.
doi:10.1016/j.jpowsour.2011.01.048

Nomenclature

$\mathcal{R}_C$	the rate of carbon monoxide oxidation, as modeled using an empirical rate law
$\mathcal{R}_H$	the rate of hydrogen oxidation, as modeled using an empirical rate law
$\mathcal{R}_L$	the rate of carbon monoxide oxidation, as modeled using a mechanistic (Langmuir–Hinshelwood-type) rate law
$\mathcal{R}_D$	the rate at which the water–gas-shift reaction occurs
k_C	the pre-exponential rate constant (parameter) appearing in $\mathcal{R}_C$
k_H	the pre-exponential rate constant (parameter) appearing in $\mathcal{R}_H$
$k_{L,1}$	the pre-exponential rate constant (parameter) appearing in the numerator of $\mathcal{R}_L$
$k_{L,2}$	the pre-exponential rate constant (parameter) appearing in the denominator of $\mathcal{R}_L$
k_D	the pre-exponential rate constant (parameter) appearing in $\mathcal{R}_D$
$\mathcal{K}_{eq}$	the equilibrium constant for the water–gas-shift reaction
E_C	the activation energy (parameter) appearing in $\mathcal{R}_C$
E_H	the activation energy (parameter) appearing in $\mathcal{R}_H$
$k_{L,1}$	the activation energy (parameter) appearing in the numerator of $\mathcal{R}_L$
$k_{L,2}$	the activation energy (parameter) appearing in the denominator of $\mathcal{R}_L$
k_D	the activation energy (parameter) appearing in $\mathcal{R}_D$
a	the order (parameter) of $\mathcal{R}_C$ with respect to carbon monoxide
b	the order (parameter) of $\mathcal{R}_C$ with respect to oxygen
c	the order (parameter) of $\mathcal{R}_H$ with respect to oxygen
$\mathcal{C}_{CO}$	the local concentration of carbon monoxide
$\mathcal{C}_{O_2}$	the local concentration of oxygen
$\mathcal{C}_{H_2O}$	the local concentration of water vapor
R	the universal gas constant.
T	temperature
$\mathcal{A}$	the cross-sectional area of the continuous-flow reactor
$\mathcal{V}$	the superficial flow velocity of the reaction mixture
$\mathcal{Q}$	the space-velocty of the reaction mixture. Calculated as $\mathcal{V}/L$
$\mathcal{F}$	the estimator function
$\mathcal{P}$	the set of parameter values to be estimated
$\mathcal{M}$	the number of operating temperatures for which conversion or selectivity data is available
$\mathcal{X}_k$	the conversion achieved by the catalyst operating at temperature T_k
$\mathcal{S}_k$	the oxidative selectivity achieved by the catalyst operating at temperature T_k
$R_{\mathcal{X}}$	the coefficient of determination for the model fitting of conversion data
$R_{\mathcal{S}}$	the coefficient of determination for the model fitting of selectivity data

achieved, and their selectivity towards CO oxidation versus H_2 oxidation. To do so, we first formulate a general dynamic material balance model describing a gas-phase isothermal plug-flow-reactor (PFR) typical of those commonly used in such processes. Then, four different kinetic (rate) models are developed, based upon use of an emprical or mechanistic approach, with and without the simultaneous participation of a water–gas-shift reaction. Finally, using our parameter estimation technique, each kinetic model is fit to the experimental conversion and selectivity measurements taken from several reports in the recent literature.

We close by evaluating the effectiveness by which each model recaptures catalyst performance, discussing the significance of the water–gas-shift reaction within PROX processes, and attempting to identify any evident kinetic parameter trends according to the active catalyst component.

2. Computational methods

2.1. Reactor model

Classically, the preferential oxidation of CO considers the simultaneous catalysis of two reactions:

$$CO + \frac{1}{2}O_2 \rightarrow CO_2 \quad \Delta H^{\circ}_{298} = -283.0 \ \text{kJ mol}^{-1}, \tag{1}$$

$$H_2 + \frac{1}{2}O_2 \rightarrow H_2O \quad \Delta H^{\circ}_{298} = -241.8 \ \text{kJ mol}^{-1}. \tag{2}$$

The kinetics of these two reactions have been modeled in the literature [2,4,5] using generalized empirical rate laws of the form:

$$R_C = k_C \exp\left(-\frac{E_C}{RT}\right) C_{CO}^{a} C_{O_2}^{b}, \tag{3}$$

$$R_H = k_H \exp\left(-\frac{E_H}{RT}\right) C_{O_2}^{c}. \tag{4}$$

It has been shown [6–8] that the apparent rate of the hydrogen oxidation reaction is independent of the local hydrogen concentration, and hydrogen is therefore omitted from Eq. (4).

The catalytic oxidation of carbon monoxide is generally believed to proceed through a surface-reaction mechanism, which has prompted a number of researchers to model the kinetics of reaction 1 using more mechanistically oriented rate laws [9–11]. One such law, examined by Venderbosch and co-workers [12], follows a Langmuir–Hinshelwood (LH) type mechanism:

$$R_L = \frac{k_{L,1} \quad \exp(-(E_{L,1}/\text{RT}))C_{CO}C_{O_2}}{(1 + k_{L,2} \quad \exp(-(E_{L,2}/\text{RT}))C_{CO})^2}. \tag{5}$$

Additionally, it has been suggested [2] that the water–gas-shift (WGS) reaction can occur under the conditions present within a typical PROX reactor.

$$H_2O + CO \leftrightarrow CO_2 + H_2 \quad \Delta H^{\circ}_{298} = -41.1 \ \text{kJ mol}^{-1}, \tag{6}$$

More specifically, large amounts of hydrogen and carbon dioxide commonly present in the reactant gas stream could promote the reverse of reaction (6), wherein carbon monoxide is regenerated. It has been shown [13] that the kinetics of this process are well described using the following rate law:

$$R_D = k_D \quad \exp\left(-\frac{E_D}{RT}\right)\left(C_{CO}C_{H_2O} - \frac{C_{CO_2}C_{H_2}}{\mathcal{K}_{eq}}\right). \tag{7}$$

The equilibrium constant of the WGS reaction is known to be well estimated as: $\mathcal{K}_{eq} = \exp\ ((4577.8/T) - 4.33)$ [14].

The typical configuration for a PROX reactor is a fixed-bed tubular continuous-flow system. For any chemical species i reacting within such a system, the material balance for i surrounding an ∂z-thick axial segment of the reactor can be constructed as follows:

$$\frac{\partial}{\partial t}(C_i \mathcal{A} \partial z) = R_i \mathcal{A} \partial z + \mathcal{A}(VC_i\big|_z - VC_i\big|_{z+\partial z}). \tag{8}$$

C_i is the local molar concentration of species i, $\mathcal{A}$ is the cross-sectional area of the reactor, R_i is the kinetic rate law describing the consumption or generation of species i, and V is the local superficial flow velocity of the reacting mixture.

Table 1
Expressing the rate at which each individual species is consumed or generated, for each kinetic model, as a stoichiometric sum of reaction rates. $\mathcal{R}_C$ is described in Eq. (3), $\mathcal{R}_H$ in Eq. (4), $\mathcal{R}_L$ in Eq. (5), and $\mathcal{R}_D$ in Eq. (7).

Rate	Kinetic model			
	Empirical	Empirical + WGS	Mechanistic	Mechanistic + WGS
$\mathcal{R}_{CO}$	$-\mathcal{R}_C$	$-\mathcal{R}_C - \mathcal{R}_D$	$-\mathcal{R}_L$	$-\mathcal{R}_L - \mathcal{R}_D$
$\mathcal{R}_{CO_2}$	$\mathcal{R}_C$	$\mathcal{R}_C + \mathcal{R}_D$	$\mathcal{R}_L$	$\mathcal{R}_L + \mathcal{R}_D$
$\mathcal{R}_{H_2}$	$-\mathcal{R}_H$	$-\mathcal{R}_H + \mathcal{R}_D$	$-\mathcal{R}_H$	$-\mathcal{R}_H + \mathcal{R}_D$
$\mathcal{R}_{H_2O}$	R_H	$\mathcal{R}_H - \mathcal{R}_D$	$\mathcal{R}_H$	$\mathcal{R}_H - \mathcal{R}_D$
R_{O_2}	$1/2(-\mathcal{R}_C - \mathcal{R}_H)$	$1/2(-\mathcal{R}_C - \mathcal{R}_H)$	$1/2(-\mathcal{R}_C - \mathcal{R}_H)$	$1/2(-\mathcal{R}_C - \mathcal{R}_H)$
Kinetic parameters	7	9	7	9

The particular R_i for each reacting species within the PROX system depends upon the particular rate laws chosen to model the reaction system. As we have discussed, there is support in the literature for the modeling of carbon monoxide oxidation using both the generic empirical rate law given in Eq. (3), and more mechanistic rate laws such as that given in Eq. (5). It is also not clear to what extent the WGS (or reverse WGS) reaction is in fact active within the PROX reactor. For these reasons, in the present investigation, we chose to consider four alternate possible cases for each R_i. These correspond to the use of empirical or mechanistic rate laws describing carbon monoxide oxidation, each with or without simultaneous participation of the WGS reaction. The appropriate R_i's, expressed as the proper stoichiometric sum of rate laws, are shown in Table 1.

Under steady-state conditions, Eq. (8) neatly simplifies to:

$$\frac{d}{dz}(VC_i) = R_i. \tag{9}$$

Rigorously, the magnitude of the local flow velocity depends upon the local temperature, pressure, and molar density of the reaction mixture. Of these three, temperature is generally of least concern for modeling purposes since PROX reactors are customarily operated under isothermal conditions. Furthermore, pressure drops due to flow through the catalytic bed are typically quite small (<5 kPa [5], <0.1 atm [11]). It is therefore not unreasonable to assume isobaric operation. Finally, even though both oxidation reactions cause a net decrease in the total mole count, the overall effect of these reactions upon molar density within the reactor is minimal. This is because both the total amount of CO entering the reactor (≈1%), and the overall extent of H_2 oxidation are usually each quite small.

As a result, we assume that the flow velocity within the reactor may be considered constant.

Knowing this, and making a substitution in variables ($q = z/L$, where L is the length of the tubular reactor) we may re-express Eq. (9) as:

$$\left(\frac{\mathcal{V}}{L}\right)\frac{d}{dq}\mathcal{C}_i = R_i \Rightarrow \frac{d\mathcal{C}_i}{dq} = \frac{1}{\mathcal{Q}}R_i. \tag{10}$$

This alternative representation of the material balance is advantageous for modeling, as it is independent of specific reactor geometry. The variable q is a dimensionless fraction of overall reactor length ($0 \le q \le 1$), and the quantity $V/L = Q$ is the space velocity of gases within the reactor (i.e. the number of reactor volumes processed per unit time).

This material balance makes additional implicit assumptions: (1) that the flow velocity is sufficently large such that convective mass transfer dominates any diffusive mass transfer processes along the long axis of the reactor, (2) that this velocity is uniform over the cross-section of the reactor, and (3) that flow is sufficiently turbulent so as to cause perfect mixing in the radial (non-axial) dimension. In general, all three of these assumptions are valid for reactors operating under sufficiently high space velocities (>1 volume per second).

2.2. Basis for parameter estimation

The usefullness of any mathematical model hinges upon its ability to accurately represent real systems. For the model we have just described to accurately represent real PROX systems, we are faced with the need to identify suitable values for those parameters ($\mathcal{P}$) appearing in the rate laws.

We previously described the use of a straight-foward general-purpose optimization-based technique for the estimation of unknown parameter values, applied to dynamic models of cell metabolism [1]. The technique applies numerical discretization techniques to convert differential equations comprising the model of interest into an approximating set of purely algebraic expressions. The discretized expressions are then used to constrain an optimization problem whose objective is to minimize the error between system performance as predicted by the model against that observed experimentally.

Numerically discretizing a generic function ϑ assumes that when given a particular function value corresponding to a particular independent variable value (q), then the function value at a different arbitrary value of the independent variable ($q + \delta q$) can be estimated using an algebraic relationship of the form:

$$\vartheta\big|_{q+\delta q} - \vartheta\big|_q = \mathcal{F}\left(\vartheta, q, \delta q\right). \tag{11}$$

The nature of the estimator $\mathcal{F}$ defines the chosen discretization method. Arguably the simplest discretization technique is the explicit first-order Euler method, wherein $\mathcal{F} \equiv d\vartheta/dq\big|_q \delta q$. Although quite straight-forward, estimates generated using this method can occasionally have substantial error.

From the fundamental theorem of the calculus, it is known that:

$$\vartheta\big|_{q+\delta q} - \vartheta\big|_q = \int_q^{q+\delta q} \frac{d\vartheta}{dq} dq. \tag{12}$$

Comparing Eq. (12) against Eq. (11) it is clear that a perfect estimator $\mathcal{F}$ precisely calculates the area under the curve $d\vartheta/dq$ between q and $q + \delta q$. When using an explicit first-order Euler estimator, the left-hand panel of Fig. 1 shows the potentially large difference (error) between the estimated and actual values of this area for a generic $d\vartheta/dq$. The right-hand panel of this figure, however, shows how the calculation can be improved using a simple second-order trapezoidal estimator: $\mathcal{F} \equiv 1/2(\, d\vartheta/dq\big|_q + d\vartheta/dq\big|_{q+\delta q})\delta q$. This approach, a second-order Runge–Kutta method, is sometimes called Heun's method.

Because of the potential for reduction in estimation error offered with only a minor increase in computational complexity, this second-order method was chosen for the present parameter estimation.

2.3. Parameter estimation problem formulation

The performance of a PROX catalyst is typically measured by the carbon monoxide conversion ($\mathcal{X}_k = \mathcal{C}_{CO}|_{0,T_k} - \mathcal{C}_{CO}|_{1,T_k}/\mathcal{C}_{CO}|_{0,T_k}$)

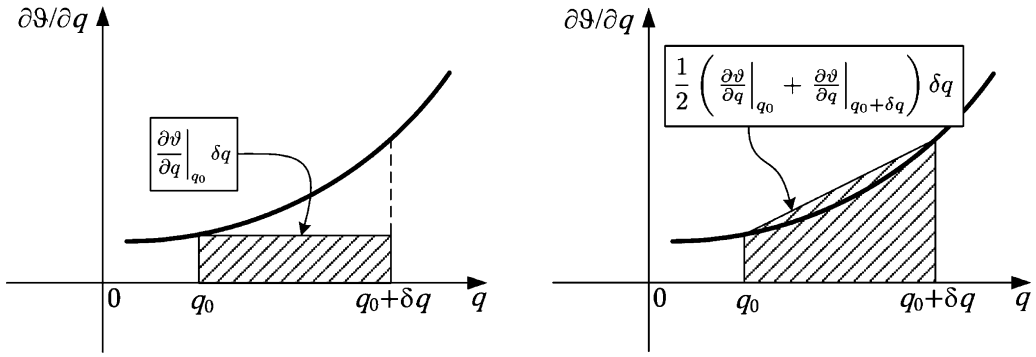

Fig. 1. Illustrating the potential reduction in error by using a simple second-order estimator.

and oxidative selectivity ($S_k = 1/2((\mathcal{C}_{CO}|_{0,T_k} - \mathcal{C}_{CO}|_{1,T_k})/(\mathcal{C}_{O_2}\big|_{0,T_k} - \mathcal{C}_{O_2}\big|_{1,T_k}))$) achieved at a particular operating temperature T_k. We therefore wish our model to reproduce real (observed) conversion and selectivity values as closely as possible. Mathematically, we phrase this goal as maximizing the quantity:

$$R^2_{\mathcal{X}} + R^2_{\mathcal{S}}, \tag{13}$$

where

$$R^2_{\mathcal{X}} = 1 - \frac{\sum_{k=1}^{\mathcal{M}}(\mathcal{X}_k - \mathcal{X}^\circ_k)^2}{\sum_{k=1}^{\mathcal{M}}(\overline{\mathcal{X}}^\circ - \mathcal{X}^\circ_k)^2}, \tag{14}$$

and similarly for $R^2_{\mathcal{S}}$.

Each R^2 quantity is a coefficient of determination, measuring the quality by which conversion and selectivity value estimated using the kinetic parameters in our model ($\mathcal{X}_k$ and $\mathcal{S}_k$) capture the variation in the experimentally observed data ($\mathcal{S}^\circ_k$, $\mathcal{S}^\circ_k$), as compared to simply using the experimental mean ($\overline{\mathcal{X}}^\circ_k$, $\overline{\mathcal{S}}^\circ_k$) as the estimate. $\mathcal{M}$ is the number of distinct temperatures for which conversion and selectivity data have been observed.

For any particular temperature T_k, the discretized material balance for species i is represented using the second-order estimator as follows:

$$\mathcal{C}_i\big|_{q_{j+1},T_k} - \mathcal{C}_i\big|_{q_j,T_k} = \frac{1}{2\mathcal{Q}}(\mathcal{R}_i\big|_{q_j,T_k} + \mathcal{R}_i\big|_{q_{j+1},T_k})\delta q \qquad \begin{matrix} \forall i \in \{CO, CO_2, H_2, H_2O, O_2\} \\ \forall j \in Z, \quad 0 \le j \le \mathcal{N}-1 \\ \forall k \in Z, \quad 1 \le k \le \mathcal{M} \\ C_i\big|_0 = C^\circ_i \end{matrix}, \tag{15}$$

$\mathcal{N}$ is the number of locations within the reactor for which concentration data is estimated. Consequently, $\delta q = 1/\mathcal{N} = q_{j+1} - q_j$, and $q_0 = 0$. C°_i is the experimentally reported inlet concentration of species i (i.e. at $q = 0$).

Our overall parameter estimation problem is concisely stated as follows:

$$\min_{\mathcal{P}} [\text{Eq. (12)}] \quad \text{subject to : [Eq. (15)]}, \tag{16}$$

This is a highly non-linear (and non-convex) mathematical program, and is best solved using numerical optimization techniques. For this investigation, all such parameter estimation problems were solved using the IPOPT optimization algorithm developed by Wächter and Biegler [15].

2.4. Case-studies

To demonstrate the flexibility and utility of our parameter estimation technique, we applied the method to estimate kinetic parameters for PROX catalysts described in eight different investigations taken from the recent literature. The chosen investigations are summarized in Table 2, and cover a variety of catalyst formulations commonly found in practice (e.g. supported platinum, copper/copper-oxide, gold, and ruthenium) [16].

All of the investigations chosen report experimentally observed values for carbon monoxide conversion as a function of temperature ($\mathcal{X}^\circ_k$). The number of distinct conversion values reported (and thus the number of distinct operating temperatures considered) in each investigation is listed in the table ($\mathcal{M}$). Additionally, the inlet gas feed composition (i.e. C°_i) and operating space velocity ($\mathcal{Q}$) are also listed for each investigation.

Not every investigation we considered provided values for the oxidative selectivity of their catalyst ($\mathcal{S}^\circ_k$). These investigations are indicated in Table 2. In such cases, kinetic parameters were estimated on the basis of $R^2_{\mathcal{X}}$ only. Finally, some investigations also report kinetic parameters for their catalyst formulation, estimated using a method of their own choosing. For each such case, the parameter values obtained using our technique are compared against those using the original authors' technique(s) as part of our discussion.

3. Results and discussion

In Table 3, we report values of $R^2_{\mathcal{X}}$ and $R^2_{\mathcal{S}}$ obtained by fitting the conversion and selectivity measurements reported for the catalysts in each of the eight chosen investigations using parameters estimated through our approach for each of the four kinetic models described previously. To more clearly visualize these results, we have prepared Fig. 2. Here, values of conversion and selectivity resulting from parameter estimation using the kinetic model identified in Table 3 to provide the highest quality fit are plotted against the conversion and selectivity values taken from the original studies. The identity function is included in each plot as an ideal reference.

In many cases using models considering WGS activity, it was found that the most optimal fit of the observed data was obtained when the WGS reaction was in fact predicted to be inactive (i.e. k_D was estimated to be zero, or E_D was estimated to be

Table 2
Summary of the eight recent literature investigations considered in this study.

Reference	Catalyst	Feed composition[a]	$\mathcal{M}$	$\mathcal{Q}$	Selectivity?	Parameters?
[4]	1% Pt on mordenite	1%CO, 20%CO_2, 40%H_2, 1.5%O_2	11	10,000 h^{-1}	No	Yes
[2]	0.5% Pt/0.02% Fe, on alumina	1%CO, 22%CO_2, 72%H_2, 1%O_2	8	260 h^{-1}	Yes	Yes
[20]	0.38% Pt/10.56% Mn, on alumina	1%CO, 60%H_2, 1%O_2	6	12,000 h^{-1}	Yes	Yes
[23]	0.50% Pt on alumina	1%CO, 20%CO_2, 50%H_2, 20%H_2O, 1%O_2	11	10,000 h^{-1}	Yes	No
[17]	15% CuO on ceria	0.03%CO, 1%H_2, 0.03%O_2	6	83,000 h^{-1}	Yes	Yes
[18]	5% CuO on ceria/zirconia	0.49%CO, 23.26%CO_2, 74.17%H_2, 0.61%O_2	5	5000 h^{-1}	No	No
[21]	0.5% Ru on alumina	0.5%CO, 18%CO_2, 37%H_2, 5%H_2O, 0.5%O_2	5	67,000 h^{-1}	Yes	No
[19]	2% Au on thoria	1%CO, 48%H_2, 1%O_2	7	6000 h^{-1}	No	No

[a] The balance of the indicated feed consists of inert materials.

Table 3
Coefficients of determination ($R^2_{\mathcal{X}}$, R^2_S) listed by study and kinetic model. Best fit (largest $R^2_{\mathcal{X}} + R^2_S$) for each study is highlighted in boldface.

Reference	Kinetic model			
	Empirical	Empirical + WGS	Mechanistic	Mechanistic + WGS
[4]	(0.986[a])	–[b]	**(0.996[a])**	–[b]
[2]	(0.962, 0949)	**(0.970, 0.956)**	(0.904, 0.893)	–[b]
[20]	**(0.743, 0.753)**	–[b]	(0.519, 0.860)	–[b]
[23]	**(0.921, 0.697)**	–[b]	(0.663, 0876)	–[b]
[17]	**(0.981, 0.911)**	–[b]	(0.978, 0.903)	–[b]
[18]	(0.887[a])	**(0.972[a])**	**(0.972[a])**	–[b]
[21]	**(0781, 0.673)**	–[b]	(0.597, 0.741)	–[b]
[19]	**(0.999[a])**	–[b]	(0998[a])	–[b]

[a] Because no selectivity data was reported in the referenced study, R^2_S was not calculated or used as a basis for parameter estimation.
[b] Optimal solution has zero WGS activity.

prohibitively large). In such cases, the model is kinetically identical to the associated basic model (where no WGS activity was considered). Consequently, no results are entered for such cases in Table 3.

Table 4, shows the kinetic parameter values obtained through estimation for each (non-empty) case shown in Table 3. Wherever possible, parameter values reported in the original referenced study are included beneath our estimated values for comparison.

From our results, it is first apparent that in most cases the empirical models we considered provide equivalent or better fitting of observed catalyst performance than do the mechanistic models. In fact, in only one case ([4]) is it shown that a mechanistic

Table 4
Estimated kinetic parameter values listed by study and kinetic model. Where available, comparison parameters for a given study are included in *italics*. Activation energies (E_C, E_H, E_D, $E_{L,1}$, and $E_{L,2}$) are reported in kJ mol^{-1}. k values are reported in the following units, k_C: $1/s\ (\text{mol m}^{-3})^{1-(a+b)}$, k_H: $1/s\ (\text{mol m}^{-3})^{1-c}$, k_D: $1/s\ (\text{mol m}^{-3})^{-1}$, $k_{L,1}$: $1/s$, $k_{L,2}$: $1/s\ (\text{mol m}^{-3})^{-1}$. Exponents ($a$, b, and c) are unitless.

Reference	$(R^2_{\mathcal{X}}, R^2_S)$	k_C	E_C	k_H	E_H	a	b	c
Kinetic model: empirical								
2*[4]	2*(0.986)	5.17×10^5	31.41	1.03×10^7	44.67	0.78	0.71	1.20
		–[a]	*40.1*	–[a]	–[a]	*−0.69*	*0.68*	–[a]
[2]	(0962,0.949)	38.95	29.40	1.23×10^7	55.87	−0.78	0.82	3.00
2*[20]	2*(0743, 0.753)	8.76×10^6	46.61	2.85×10^7	55.44	−1.31	3.00	0.95
		–[a]	*58.1*	–[a]	*101.8*	–[a]	–[a]	–[a]
[23]	(0.921, 0.697)	1.14×10^6	48.44	3.88×10^7	56.97	−0.73	1.29	1.20
2*[17]	2*(0.981, 0.911)	1.88×10^7	29.86	3.26×10^5	60.41	0	2.02	0
		–[a]	*48.5*	–[a]	–[a]	–[a]	–[a]	–[a]
[18]	(0.887)	4.08×10^5	40.74	1.34	0.53	0.97	0	0.52
[21]	(0.781, 0.673)	1.33×10^6	35.56	3.34×10^7	49.10	0.01	1.07	0.92
[19]	(0.999)	4.90×10^4	26.75	4.93×10^5	29.31	−1.07	1.34	1.09

Reference	$(R^2_{\mathcal{X}}, R^2_S)$	k_C	E_C	k_H	E_H	k_D	E_D	a	b	c
Kinetic model: empirical + WGS										
2*[2]	2*(0970, 0.756)	0.246	14.65	758.8	28.89	1.86×10^5	81.93	−1.39	0.79	1.65
		352.8	*33.09*	*20.53*	*18.74*	*4402*	*34.10*	*−0.10*	*0.50*	*0.50*
[18]	(0.972)	1.93×10^5	41.51	3.99×10^{-3}	0.13	1.58×10^4	40.79	0.29	0.33	2.97

Reference	$(R^2_{\mathcal{X}}, R^2_S)$	$k_{L,1}$	$E_{L,1}$	$k_{L,2}$	$E_{L,2}$	k_H	E_H	C
Kinetic model: mechanistic								
[4]	(0.996)	5.72×10^4	15.02	4.16×10^{-3}	1.96×10^{-5}	1341.04	14.59	1.10
[2]	(0.904, 0.893)	4.55×10^6	59.64	2.60×10^7	110.75	2.23×10^6	54.48	2.08
[20]	(0.519, 0.860)	1.06×10^6	37.43	0	0	5.42×10^7	57.68	0.99
[23]	(0.663, 0.876)	6.71×10^5	37.91	1.21×10^4	71.41	2.68	5.98	0
[17]	(0.978, 0.903)	1.95×10^8	36.76	0	0	9.21×10^4	55.78	0
[18]	(0.972)	5.09×10^6	29.62	1.80×10^{-2}	1.90×10^{-7}	1.82×10^6	49.48	0.81
[21]	(0.597, 0.741)	4.62×10^7	39.73	0	0	1.54×10^7	46.72	0.90
[19]	(0.998)	3.36×10^6	21.26	8.19×10^{-3}	7.91×10^{-6}	5583.56	25.45	0.92

[a] No value for the indicated parameter was provided in the referenced study.

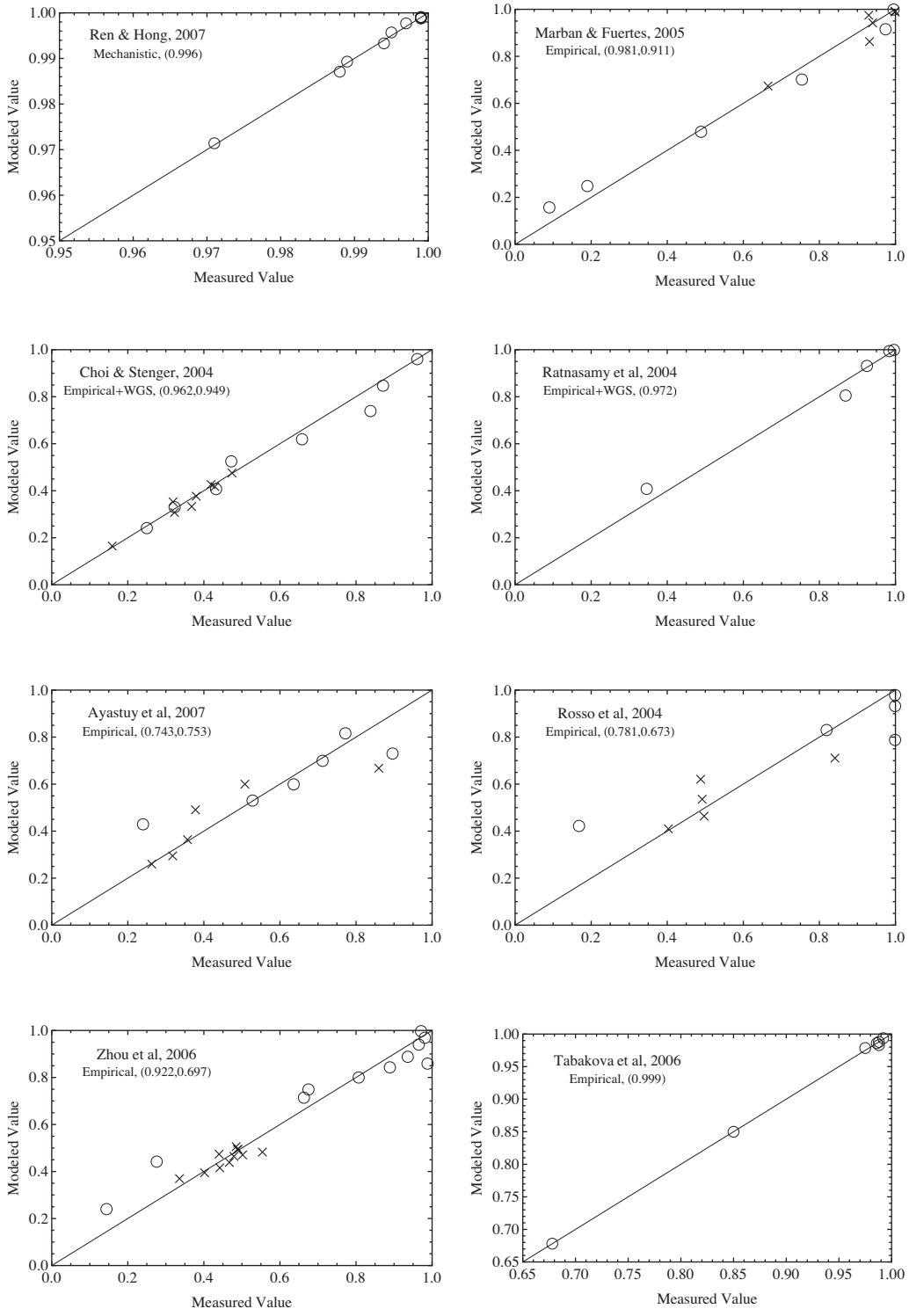

Fig. 2. Visualization of fitting quality for each chosen study. Conversion (○) and selectivity (×) values taken from the original study are plotted along the horizontal axis ("measured value"); values obtained through parameter estimation are plotted along the vertical axis ("modeled value"). The particular kinetic model used, and the resulting values of (R^2_X, R^2_S) are indicated in each panel.

model provides a marginally better approximation of catalyst performance.

Mechanistic models, when they can be fit to observed performance data, usually generate parameter values more closely tied to the underlying chemistry, and thus can offer more detailed insight than can general-purpose empirical models. Often however, such detailed information is not needed for process engineering applications where it is more important to accurately model macroscopic catalyst and reactor performance than it is to accurately model microscopic surface interactions between reactants and catalyst. Moreover, if a model based upon an inappropriate surface-reaction mechanism is chosen, it may be impossible to

accurately model the catalyst performance and/or the parameter values obtained may not characterize the underlying chemistry as accurately as is hoped.

For five of our chosen studies ([4,2,17–19]), the mechanistic model we have chosen – based upon a bi-molecular LH surface mechanism – provides a good approximation of the overall catalyst performance ($R^2_{\mathcal{X}} > 0.9$, $R^2_{\mathcal{S}} \approx 0.9$). For the remaining three studies, however, this model is apparently ill-suited to the catalyst.

We also note that in two cases ([20,21]), neither model (emprical or mechanistic) appears capable of generating parameters that very accurately describe the observed catalyst performance ($R^2_{\mathcal{X}} \approx 0.75$, $R^2_{\mathcal{S}} \approx 0.7$). Although the empirical model still offers the better fit in each case, the results suggest that a better solution might be achievable using a kinetic model not considered here. While it is generally well accepted that the oxidation of CO proceeds via an LH-type mechanism over Pt [12], the catalyst formulations described in these two studies are based upon Ru [21] and a Pt/MnO_x blend [20]. It is therefore not unreasonable to expect that their surface chemistries may follow different models.

In general, unless a precise reaction mechanism is known, there appears to be little practical advantage in modeling the catalytic oxidation of CO using mechanistic models (over general empirical models) for process engineering applications.

The results in Table 3 also provide some insight into the role of the WGS reaction within PROX reactors. In most cases, the best fit of the experimental conversion and selectivity data is obtained when this reaction is inactive. In these cases, therefore, the observed conversion and selectivity is adquately explained through catalysis of the principal CO and H_2 oxidation reactions only. For two of our chosen studies, however, the best fit to observed catalyst performance is obtained with non-zero WGS activity.

Choi and Stenger [2] reported that WGS activity was expected to be most significant under conditions where large amounts of H_2 and CO_2 are present in the feed, overwhelming the forward reaction as favored by chemical equilibrium. It is therefore not surprising that the two cases for which non-zero WGS activity was predicted involve feed streams containing at least 90% H_2/CO_2. Our results are therefore consistent with the expectations of Choi and Stenger, and demonstrate that simultaneous catalysis of the WGS reaction must be considered when feeding PROX with a large amounts of H_2 or CO_2.

Examining the parameter values given in Table 4, we first find that, in general, the activation barrier for CO oxidation (E_C) is lower than that for H_2 oxidation (E_H). This is to be expected from catalysts that preferentially oxidize CO.

Examining the parameter data further, we discover that trends in parameter values, even for catalyst preparations based upon the same active metal or metal oxide, are not immediately evident. Because the apparent chemical kinetics of a catalyst are affected not only by its active component, but also its support, its preparation method, and the operating conditions to which it is exposed [16,22] this lack of discernable trends is not discomforting.

Finally, we note that three of our chosen studies ([4,18,19]) did not report selectivity data as a function of temperature. Kinetic parameters in these cases could therefore be estimated only on the basis of CO conversion. As a result, the importance of the H_2 oxidation kinetics are de-emphasized in these cases, and we therefore have less confidence in the accuracy of the kinetic parameters K_H, E_H, and C. This is particularly true in the case of Ratnasamy et al. [18] for which the emipirical model estimates a value of E_H substantially less than E_C; values inconsistent with the preferential oxidation of CO.

Acknowledgements

This work was supported in part through the Integrative Graduate Education and Research Traineeship (IGERT) for Fuel-Cell Technology at Rensselaer Polytechnic Institute (NSF Award Number DGE-0504361).

References

[1] A.C. Baughman, X. Huang, S.T. Sharfstein, L.L. Martin, Computers and Chemical Engineering 34 (2) (2010) 210–222, http://linkinghub.elsevier.com/retrieve/pii/S0098135409001677.
[2] Y. Choi, H.G. Stenger, Journal of Power Sources 129 (2) (2004) 246–254, http://linkinghub.elsevier.com/retrieve/pii/S0378775303011315.
[3] A. Serov, C. Kwak, Applied Catalysis B: Environmental 90 (3–4) (2009) 313–320, http://linkinghub.elsevier.com/retrieve/pii/S0926337309001246.
[4] S. Ren, X. Hong, Fuel Processing Technology 88 (4) (2007) 383–386, http://linkinghub.elsevier.com/retrieve/pii/S0378382006001755.
[5] D.H. Kim, J.E. Cha, Catalysis Letters 86 (1–3) (2003) 107–112.
[6] J.A. Maymo, J.M. Smith, AIChE Journal 12 (5) (1966) 845–854, http://doi.wiley.com/10.1002/aic.690120505.
[7] K. Hansen, Chemical Engineering Science 31 (7) (1976) 579–586, http://linkinghub.elsevier.com/retrieve/pii/0009250976800218.
[8] L. Verheij, Surface Science 371 (1) (1997) 100–110, http://linkinghub.elsevier.com/retrieve/pii/S0039602896009764.
[9] W. Liu, Journal of Catalysis 153 (2) (1995) 317–332, http://linkinghub.elsevier.com/retrieve/doi/10.1006/jcat.1995.1133.
[10] G. Sedmak, Journal of Catalysis 213 (2) (2003) 135–150, http://linkinghub.elsevier.com/retrieve/pii/S0021951702000192.
[11] T. Caputo, L. Lisi, R. Pirone, G. Russo, Industrial and Engineering Chemistry Research 46 (21) (2007) 6793–6800, http://pubs.acs.org/doi/abs/10.1021/ie0616951.
[12] R. Venderbosch, Chemical Engineering Science 53 (19) (1998) 3355–3366, http://linkinghub.elsevier.com/retrieve/pii/S0009250998001511.
[13] Y. Choi, Journal of Power Sources 124 (2) (2003) 432–439, http://linkinghub.elsevier.com/retrieve/pii/S0378775303006141.
[14] J. Moe, Chemical Engineering Progress 58 (1962) 33–36.
[15] A. Wächter, L.T. Biegler, Mathematical Programming 106 (1) (2005) 25–57, http://www.springerlink.com/index/10.1007/s10107-004-0559-y.
[16] E. Park, D. Lee, H. Lee, Catalysis Today 139 (4) (2009) 280–290, http://linkinghub.elsevier.com/retrieve/pii/S0920586108003027.
[17] G. Marban, Applied Catalysis B: Environmental 57 (1) (2005) 43–53, http://linkinghub.elsevier.com/retrieve/pii/S0926337304006186.
[18] P. Ratnasamy, Journal of Catalysis 221 (2) (2004) 455–465, http://linkinghub.elsevier.com/retrieve/pii/S0021951703003622.
[19] T. Tabakova, V. Idakiev, K. Tenchev, F. Boccuzzi, M. Manzoli, Applied Catalysis B: Environmental 63 (1–2) (2006) 94–103, http://linkinghub.elsevier.com/retrieve/pii/S0926337305003565.
[20] J. Ayastuy, M. Gonzalezmarcos, J. Gonzalezvelasco, M. Gutierrezortiz, Applied Catalysis B: Environmental 70 (1–4) (2007) 532–541, http://linkinghub.elsevier.com/retrieve/pii/S0926337306002700.
[21] I. Rosso, M. Antonini, C. Galletti, G. Saracco, V. Specchia, Applied Catalysis B: Environmental 37 (1) (2002) 17–25, http://linkinghub.elsevier.com/retrieve/pii/S0926337301003198.
[22] N. Bion, F. Epron, M. Moreno, F. Mariño, D. Duprez, Topics in Catalysis 51 (1–4) (2008) 76–88, http://www.springerlink.com/index/10.1007/s11244-008-9116-x.
[23] S. Zhou, Z. Yuan, S. Wang, International Journal of Hydrogen Energy 31 (7) (2006) 924–933, http://linkinghub.elsevier.com/retrieve/pii/S0360319905002697.